Study for NaI(Tl) and Scintillation Fiber with 80 MeV Proton Beam Toward ESPRI Experiment at NIRS-HIMAC, RIKEN-RIBF

II. 5. Study for NaI(Tl) and Scintillation Fiber with 80 MeV Proton Beam Toward ESPRI Experiment at NIRS-HIMAC, RIKEN-RIBF

Zenihiro J.[1], Matsuda Y.[2], Sakaguchi H.[3], Takeda H.[4], Iwao Y.[1], Matsumoto H.[1], and Itoh M.[5]

[1]Department of Physics, Kyoto University
[2]Department of Physics, Tohoku University
[3]Department of Applied Physics, Miyazaki University
[4]RIKEN
[5]Cyclotron and Radioisotope Center, Tohoku University

In recent years various new phenomena in unstable nuclei such as neutron skin or halo, have been a focus of international attention. RI beam facilities of the next generation, RIKEN-RIBF, GSI-SIS100/300, RIA at USA, and so on, are being built and various experiments are planned to confirm these phenomena.

We have already succeeded in extracting the neutron density distributions in stable nuclei by using intermediate energy polarized proton elastic scattering measurements at RCNP in Osaka University.

Now we are proposing experiments of **E**lastic **S**cattering of **P**rotons with **RI** beam (**ESPRI**) at NIRS-HIMAC and RIKEN-RIBF, and developing a new detector system composed of momentum tagging and tracking counters of the RI beam (Scintillation Fibers, two MWDCs), a Solid Hydrogen Target (SHT) and a Recoil Particle Spectrometer (RPS), to measure recoil protons in the SHT scattered by RI beam. The RPS shown in Fig.1, consists of MWDCs, plastic scintillators and finally fourteen-NaI(Tl) arrays. NaI(Tl) determines the total energy of recoil protons precisely. The Scintillation Fibers installed in the secondary beam line are used to tag the momentum of the RI beam at the focal plane of the beam line. Both of them are indispensable to the measurement of inverse kinematical proton elastic scattering with the RI beam.

In order to evaluate the performances of NaI(Tl) and Scintillation Fiber we have calibrated these detectors with 77.6 MeV proton beam at CYRIC in Nov. and Dec. of 2005.

NaI(Tl)

The size of NaI(Tl) rod is 2 inches square and 18 inches long and they cover the wide range of scattered angles of RPS from about 65 to 85 degrees in laboratory system. We measure their scintillating photons with HAMAMATSU R1307 photomultiplier tubes shown in Fig. 1, 2. The requirement for NaI(Tl) is to achieve energy resolution better than 600 keV (FWHM) independent of the energies of incident recoil protons up to 130 MeV and positions of NaI(Tl) rod. Thus we need to know the energy and position dependence of each NaI(Tl) crystal. We have already tested them with 12 MeV proton beam at Tandem Van de Graaff Accelerator Lab. at Kyoto University. The energy resolutions are about 1.5% (FWHM) and the square root gain of the left and right PMTs fluctuates about 5%. At this energy protons stop at the surface of NaI(Tl) crystal (about 1mm stopping range), so it is necessary to test with higher energy proton beam, that stops deep inside the NaI(Tl) crystal.

We used a faint proton beam of E_p = 77.6 MeV for this test experiment. The beam was directly injected into NaI(Tl) after the 10 mm thick brass collimater of 5 mm in slit width. In order to change the incident beam position on NaI(Tl) rod we mounted the NaI(Tl) detector on the stage which moved with the remote controlled pulse motor. The signals from PMTs were shaped and amplified by emitter followers and spectroscopic amplifiers ORTEC 671. Amplified signals were finally converted to digital data by peak hold ADC HOSHIN C008.

If doped Tl or crystal structure of NaI(Tl) were highly uniform, scintillating photons would be attenuated in a NaI(Tl) rod approximately as an exponential function of the length from the scintillating position to PMT. The square root of the left and right gains would be almost constant, independent of its position. But in fact, since NaI(Tl) crystals have non-uniformity to some extent, we cannot neglect the variations in square root gains (~6 %) which are larger than the resolutions (~0.5%) as shown in Fig. 3, 4. We have approximated the attenuation in non-uniform crystal by a simple sum of an exponential and a Gaussian. We fitted the left and right gains to this function with 5 parameters (Fig. 5), and got the calibrated square root gains again. By using these calibrated gains we found in Fig. 6 the variations become small nearly 600 keV in full width. Table 1 shows the fitting function and parameters used in this calibration.

At ESPRI experiments by using these calibrated gains we will be able to get the high resolution (~600keV) spectra of NaI(Tl) rods independent of incident positions, and to select elastic events.

Scintillation Fiber

Gas counters such as Low pressure MWPC and PPAC are often used as a position detector at a focal plane of a RI beam line. However, beam intensity, energy and so on are very influential in these performances. Moreover, usage of the counter gas can't release from danger. To avoid such problems, we have developed a simple one-dimensional Scintillation Fiber Detector (SFD).

The design of SFD is shown in Fig. 7. 2 mm square fibers are arranged in sixty rows. The effective area is 120 mm x 50 mm. Because of the very simple structure, areas of cladding material which are about 8% of fibers become a inefficient region. If the effective area is set up perpendicular to a beam axis, the inefficiency can't be bypassed. Of course, it isn't impossible to detect the particle passed through the clad area. But it only makes the operation more complex. Then, in order to achieve an efficiency of nearly 100 %, it was suggested that SFD is tilted toward the beam axis. Because the focal plane usually isn't perpendicular to the beam axis and the more tilting, the better the position resolution becomes, this method is fit to use.

In order to make sure this expectation, we measured the relation between the tilting angle and the efficiency using 45 MeV protons. Hit patterns and timing information of SFD were measured by multi-hit TDC AMSC 64ch AMT-VME module, via Flat Panel Photomultiplier Tube (FPPMT) HAMAMATSU H8500 and amplifier-shaping-discriminator (ASD) Gnomes Design GNA-180, of which the time constant was 16 nsec and the threshold was set to –30 mV on the chip. To monitor cross talk events occurred in FPPMT, charge pulses from the dynode are measured by ADC LeCroy 2249A, via pre-amplifier, is a same amplifier of ASD, and PMT amplifier LeCroy 612A.

Efficiency curves of each tilting angles (0, 5, 10, 15, 30, 45, 60 degrees) are shown in Fig. 8. A counting rate was about 1 kHz during measurement. An efficiency of cluster multiplicity 1 (C1), means that SFD can determine hit positions without any delicate analyses, reaches nearly 100% at more than 15 degrees. Considering the cladding thickness, it can be explained an increase of the efficiency from 0 degrees to 10 degrees.

When the operation HV becomes more than 500 V, an efficiency of cluster multiplicity 2 (C2) increases. It is caused by cross talk events in FPPMT. It can be confirmed to see correlations between time widths of anode signals and charges of dynode signals. A distribution of the sum of time widths for each cluster is shown in Fig. 9. Hatched areas mean cross talk events and can be removed by this analysis. Two bumps of true hits region at 30, 45 degrees are caused by nonlinear relation between energy loss and time widths of anode signals.

From these measurements, it was confirmed SFD have nearly 100% detection efficiency. Moreover, for 60 degrees, we could get fairly good position resolution (< 1mm full width).

The response for high counting rate (10^6 Hz) and heavy ions were also examined with 390 MeV/u ^{22}Ne primary beam and its secondary beam at HIMAC and the performance didn't go down. So SFD is installed in a momentum dispersive focal plane of SB2 course of HIMAC now. Because momentum dispersion of SB2 course is 2 cm/%, we will succeed in getting good momentum resolution (<0.1%) for beam particles.

References

1) Sakaguchi H.,et al., Phys. Rev. **C57** (1998) 1749.

Table1. the parameters of fitting function (exp + Gaussian). $p_1 \times \exp\left(-\frac{x-l}{p_2}\right) + p_3 \times \exp\left(-\left(\frac{x-p_4}{p_5}\right)^2\right)$

S/N		p1	p2	p3	p4	p5
030320-7	Left	2733.68	-1624.82	265.567	80.295	126.83
	Right	2091.85	257878	1035.4	-171.75	138.36
030527-3	Left	3198.26	-1202.99	156.5	37.507	56.746
	Right	3125.99	1713.67	37.157	17.5	31.707
030527-4	Left	3654.76	-807.673	112.77	-208.76	38.875
	Right	3167.74	1559.21	53.934	37.235	33.438

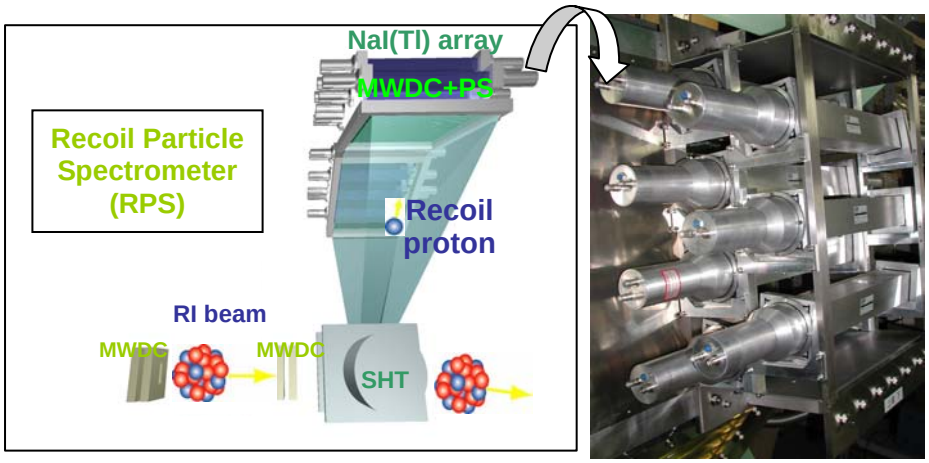

Figure 1. Schematic view of Elastic Scattering of protons with RI beam and photo of NaI(Tl) array.

Figure 2. NaI(Tl) rod of 2 x 2 x 18 inch with Hamamatsu R1307 PMT.

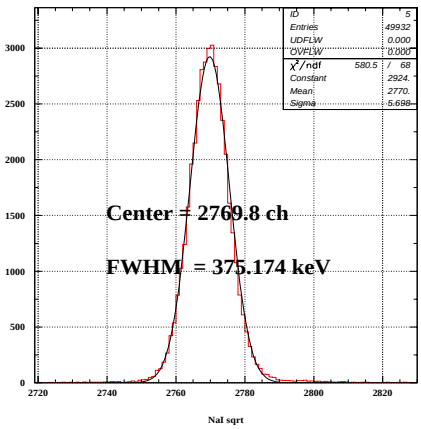

Figure 3. The resolutions at the center of a NaI(Tl) rod.

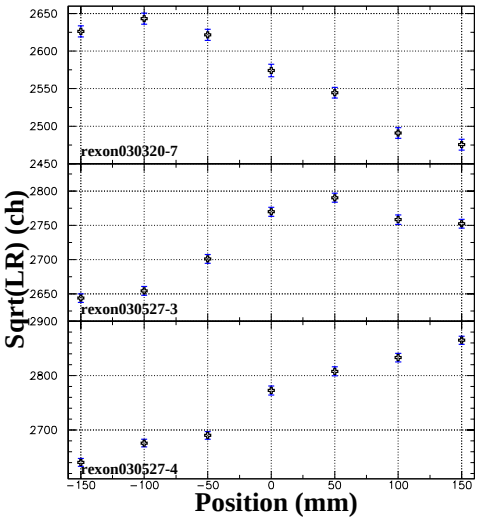

Figure 4. Gains and resolutions of each NaI(Tl) rod. While the resolutions are within 0.5% (FWHM), fluctuation of the gains is about 6%.

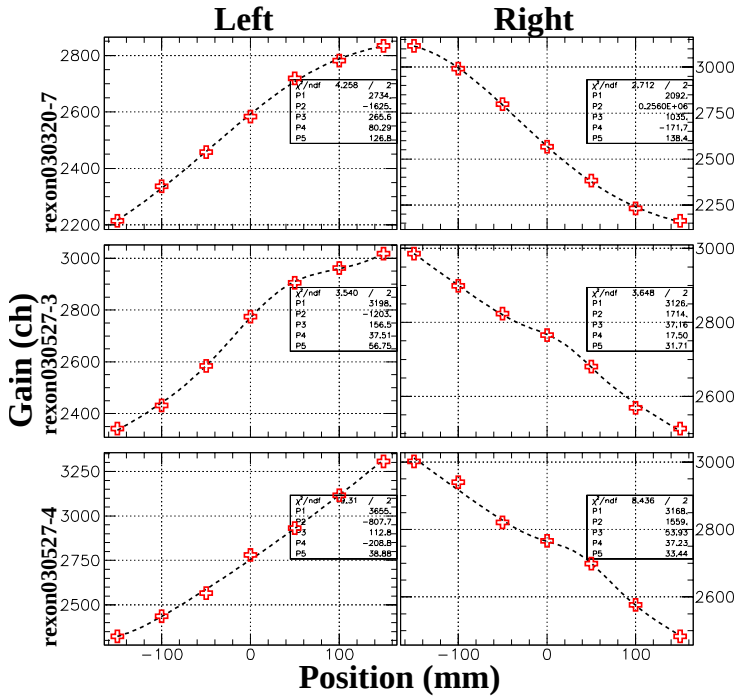

Figure 5. Left and right gains of each position in each NaI(Tl) rod. We fitted these to a function of an exponential and a Gaussian.

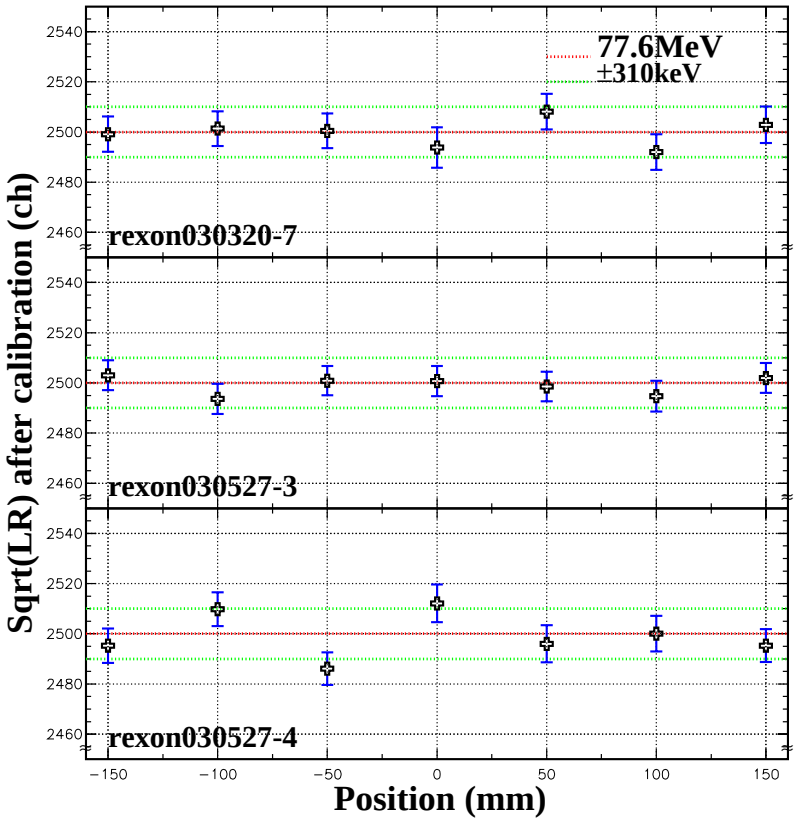

Figure 6. Each square root gains after calibration. They are within just about 600 keV in full width.

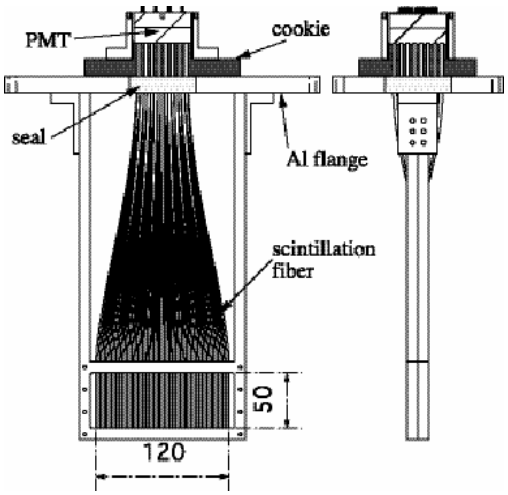

Figure 7. The schematic illustration of SFD.

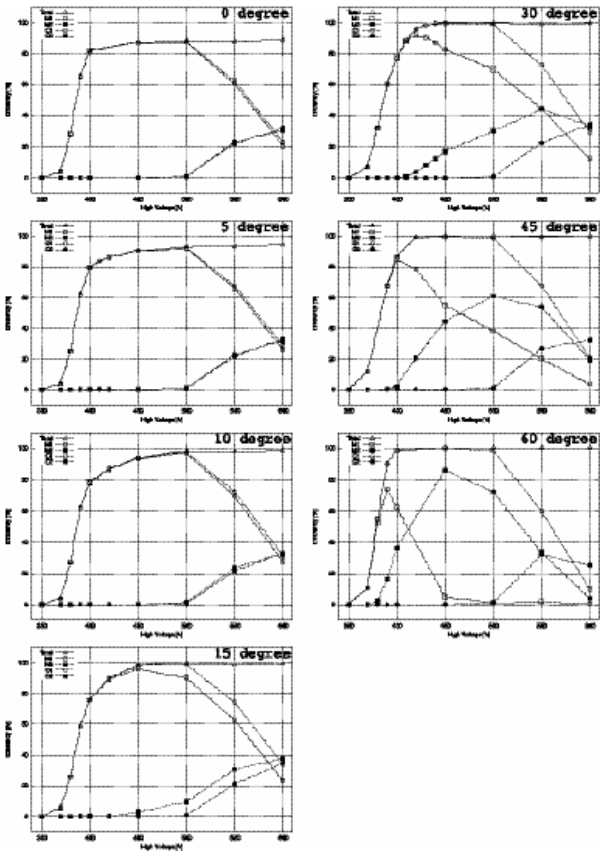

Figure 8. Efficiency curves for 45 MeV protons at various angles. Open triangles show the total efficiency: the efficiency of fiber multiplicity 1 (M1, open squares), of fiber multiplicity 2 (M2, closed circles), of cluster multiplicity 1 (C1, open circles), and of cluster multiplicity 2 (C2, closed circles).

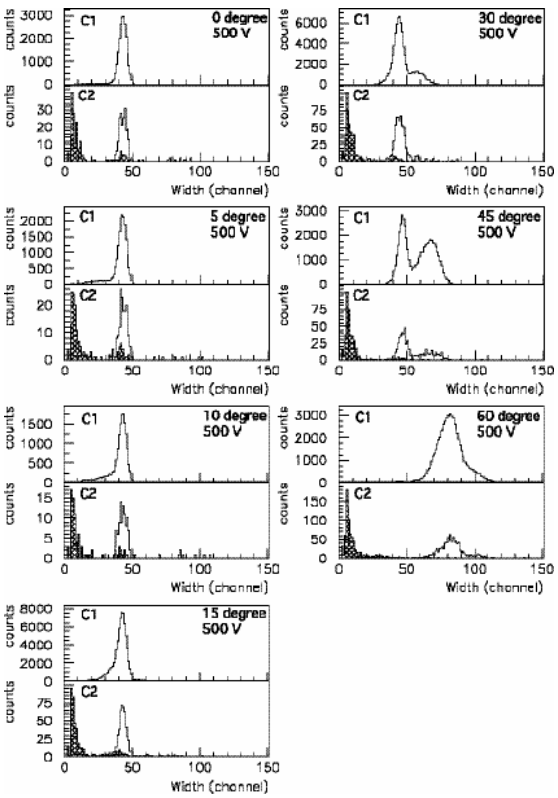

Figure 9. The distribution of the sum of time widths for each cluster. Hatched areas correspond cross talk events.